

Synthesis and Crystal Structure of ZrP_2S_6 and ZrP_2S_7

D. R. Lott, T. Fincher, G. C. LeBret, and D. A. Cleary

Department of Chemistry, Gonzaga University, Spokane, Washington 99258

and

G. L. Breneman

Department of Chemistry, Eastern Washington University, Cheney, Washington 99111

Received August 25, 1997, in revised form December 8, 1997, accepted November 17, 1998

Two new compounds have been synthesized and characterized: ZrP_2S_6 and ZrP_2S_7 . Both were prepared from direct combination of the elements at high temperature using a chemical transporting agent. Single crystal X-ray diffraction and elemental analysis (ICP-AE) were performed on the materials. ZrP_2S_6 crystallized in a tetragonal space group ($P-4$, $a = 6.6758(4)$ Å, $c = 9.491(1)$ Å) whereas the ZrP_2S_7 crystallized in a monoclinic space group ($C2/c$, $a = 8.614(1)$ Å, $b = 29.684(4)$ Å, $c = 8.583(1)$ Å, $\beta = 120.126^\circ$). The ZrP_2S_6 displayed a weak second harmonic generation at 1064 nm. © 1999 Academic Press

INTRODUCTION

The metal hexathiohypophosphates, $M_2\text{P}_2\text{S}_6$, where M is a +2 metal, have enjoyed considerable attention because of their interesting magnetic, optical, and structural properties (1). In addition, many of these compounds undergo intercalation reactions (2). Those that can be electrochemically intercalated with lithium have been investigated with respect to their utility as electrodes for secondary cells (3). We recently reported the structure and nonlinear optical properties of SnP_2S_6 (4). In SnP_2S_6 , the metal is in a formal oxidation state of +4, and therefore half the metal sites of the parent $M_2\text{P}_2\text{S}_6$ structure are vacant. This was the first report of the layered $M_2\text{P}_2\text{S}_6$ structure with a +4 metal. The goal of the work presented here was to replace the Sn^{+4} with Zr^{+4} while maintaining the acentric SnP_2S_6 structure and hence maintain the second order nonlinear optical properties.

Hahn *et al.* reported a ZrP_2S_6 phase grown at 750°C that crystallized in the centrosymmetric $P4_2/m$ space group (5). The ZrP_2S_6 phase being reported here was grown at a lower temperature (475°C) and crystallized in the acentric $P-4$ space group. The centrosymmetric and acentric structures are closely related. They differ in the Zr–S bond lengths, and

this will be discussed in detail below. The acentric ZrP_2S_6 displayed a very weak second harmonic generation at 1064 nm.

A number of compounds containing the $\text{P}_2\text{S}_7^{-4}$ ion have been reported (6–8). None contain a 1:1 pairing of the $\text{P}_2\text{S}_7^{-4}$ group and a +4 counterion. In this work we report the synthesis and structure of ZrP_2S_7 . The compound crystallized in the centrosymmetric $C2/c$ space group and did not display second harmonic generation.

EXPERIMENTAL

The ZrP_2S_6 and ZrP_2S_7 were grown from the elements. The molar ratio Zr:P:S was 2:2:6. The elements were sealed in an evacuated fused quartz ampule (150 mm long \times 22 cm ID). The tube was heated to 475°C for 10 days in a tube furnace. After 10 days, the tube was cooled and opened. A good yield of yellow needles with a square cross section (ZrP_2S_6) and orange polygons (ZrP_2S_7) was recovered from the reaction mixture. The ZrP_2S_6 needles and the ZrP_2S_7 polygons grew together at the same temperature. They were separated from each other under a microscope using tweezers.

Elemental analysis was performed on a Perkin–Elmer Optima inductively coupled plasma–atomic emission spectrometer. Samples were digested in a mixture of hydrochloric, nitric, and hydrofluoric acid using a CEM microwave digestion system. The digestions were carried out in Teflon bombs at a temperature of 150°C .

Infrared spectra were recorded on a Perkin–Elmer Spectrum 2000 Fourier-transform infrared spectrometer. Samples were prepared as KBr pellets and spectra were recorded in the transmission mode from 4000 to 400 cm^{-1} with a resolution of 4 cm^{-1} .

Second harmonic generation intensities were tested using a Continuum Nd:YAG pulse laser (Minilite). The infrared

laser wavelength was 1064 nm, the pulses were 6 nsec in duration, and the repetition rate was 10 Hz. The pulses had an energy of 31 mJ. Samples were powdered and placed between microscope slides for analysis.

Single crystal X-ray diffraction analysis was performed on an Enraf–Nonius CAD-4 diffractometer using a θ – 2θ scan. The maximum 2θ for data collection was 50° . The radiation was $\text{MoK}\alpha$ ($\lambda = 0.71073 \text{ \AA}$). An absorption correction was made for ZrP_2S_6 , but no absorption correction was necessary for ZrP_2S_7 . The structures were solved with direct methods using the SHELXTL/PC software (9). Scattering factors used were from Cromm and Mann (10).

The weights used in refinement were

$$w = \frac{1}{[\sigma^2(F) + aF^2]},$$

(where $a = 0.0005$ for ZrP_2S_6 and 0.0004 for ZrP_2S_7)

$$R = \frac{\sum |F_{\text{obs}}| - |F_{\text{calc}}|}{\sum F_{\text{obs}}},$$

and

$$wR = \sqrt{\frac{\sum (w|F_{\text{obs}}| - |F_{\text{calc}}|)^2}{\sum (wF_{\text{obs}})^2}}$$

No extinction corrections were made. Both data sets were collected at 22°C .

The ZrP_2S_6 crystal (yellow prism) was $0.2 \times 0.1 \times 0.1 \text{ mm}$. The lack of systematic extinctions led to the choices of space groups being $P4$, $P-4$, $P4/m$, $P422$, $P4mm$, $P-42m$, $P-4m2$, and $P4/mmm$. Successful refinement in $P-4$ ($R = 0.017$, $wR = 0.025$) proved this is to be the correct space group. Psi scan absorption corrections were made on this compound using an absorption coefficient of 3.73 mm^{-1} . A total of 751 reflections were measured with 733 unique reflections and 668 reflections observed ($> 3\sigma(I)$). The 668 observed reflections were used in refining 41 parameters for six atoms. The two Zr atoms were each in 1-fold special positions. Half of the P_2S_6 was in a 4-fold general position which was related to the other half by symmetry.

The ZrP_2S_7 crystal (orange) was $0.3 \times 0.15 \times 0.1 \text{ mm}$. From systematic extinctions, the choices of space groups were $C2/c$ and $C2$. Successful refinement in the centrosymmetric $C2/c$ ($R = 0.021$, $wR = 0.035$) proved this to be the correct space group. Psi scan absorption corrections were attempted on this compound, but no improvement in the final refinement was realized. Therefore, no absorption corrections were made for this compound. For ZrP_2S_7 , 1444 reflections were used in refining 92 parameters for 11 atoms. The two Zr atoms in ZrP_2S_7 were each in 4-fold special positions. A total of 1818 reflections were measured, with

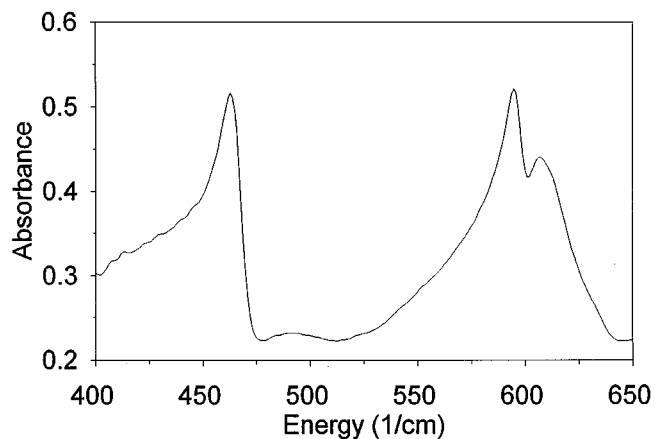


FIG. 1. Transmission infrared spectrum of ZrP_2S_6 .

1705 unique reflections and 1444 reflections observed ($> 3\sigma(I)$).

RESULTS AND DISCUSSION

The percentage of zirconium present in each sample was consistent with the stated stoichiometry, although both materials have a slight (1–3%) excess of zirconium.

The infrared spectra of ZrP_2S_6 and ZrP_2S_7 are shown in Figs. 1 and 2. The major absorption peaks for ZrP_2S_6 occur at 607 , 595 , and 463 cm^{-1} . For ZrP_2S_7 , the infrared transitions occur at 626 , 616 , 609 , 577 , 499 , and 411 cm^{-1} . The transitions are due to modes arising from $\text{P}_2\text{S}_6^{-4}$ and $\text{P}_2\text{S}_7^{-4}$, respectively (11). The $\text{P}_2\text{S}_6^{-4}$ moiety has an ethane-like (D_{3d}) point symmetry resulting in fewer observed transitions than what is observed for $\text{P}_2\text{S}_7^{-4}$, which has a point symmetry of C_1 .

The ZrP_2S_6 displayed weak second harmonic generation, and the ZrP_2S_7 did not display second harmonic generation. The second harmonic intensity of ZrP_2S_6 was much

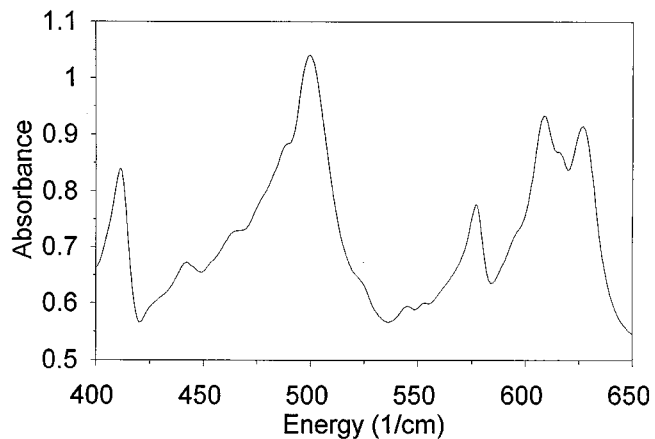


FIG. 2. Transmission infrared spectrum of ZrP_2S_7 .

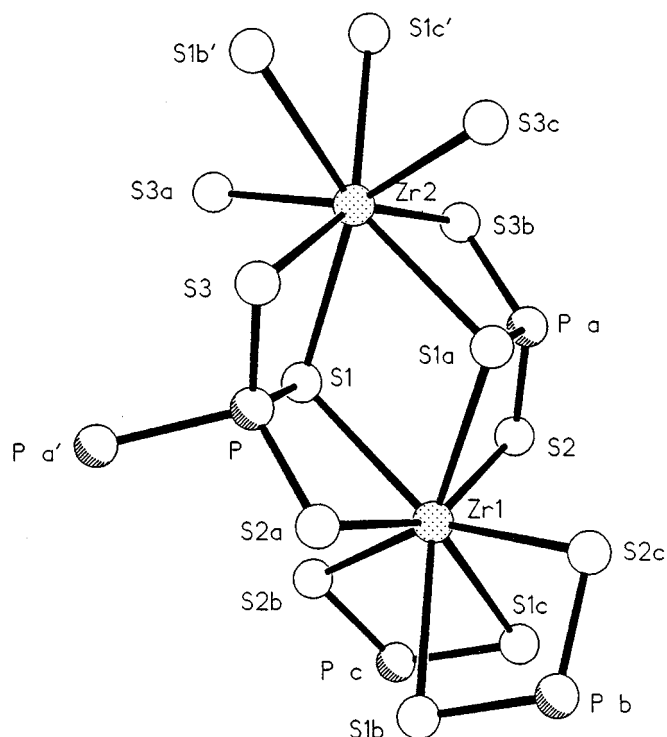


FIG. 3. Crystal structure of ZrP_2S_6 showing the coordination around the two independent Zr atoms and part of the $P_2S_6^{4-}$ ion including the atom number scheme used in Tables 1–4.

less intense than a similar sample of SnP_2S_6 . The space group $P-4$ is acentric whereas the space group $C2/c$ is centrosymmetric. The second harmonic generation results are consistent with these space groups. A lack of a center of inversion is required in order to observe second harmonic generation (12).

The coordination around the two independent Zr atoms in ZrP_2S_6 and part of the $P_2S_6^{4-}$ ion are shown in Fig. 3. The atom number scheme is consistent within Tables 1–4. The coordination around the two independent Zr atoms in ZrP_2S_7 and the $P_2S_7^{4-}$ ion are shown in Fig. 4. The atom number scheme used is consistent within Tables 5–8.

TABLE 1
Positional Parameters and Their Estimated Standard Deviations and the Equivalent Isotopic Temperature Factors ZrP_2S_6

Atom	x	y	z	B (eg)
Zr1	0.000	0.000	0.500	0.986(5)
Zr2	0.000	0.000	0.000	0.808(5)
S1	0.18361(7)	-0.15949(7)	0.2479(2)	1.066(7)
S2	0.2136(1)	0.3084(1)	0.42952(7)	1.36(1)
S3	-0.2136(1)	-0.3090(1)	0.07065(8)	1.45(1)
P	-0.05837(7)	-0.34379(7)	0.2491(2)	0.903(7)

TABLE 2
Selected Bond Distances (Å) and Their Estimated Standard Deviations for ZrP_2S_6

Atom 1	Atom 2	Distance	Atom 1	Atom 2	Distance
Zr1	S1	2.892(2)	Zr2	S1b'	2.859(2)
Zr1	S1a	2.892(2)	Zr2	S1c'	2.859(2)
Zr1	S1b	2.892(2)	Zr2	S3	2.596(2)
Zr1	S1c	2.892(2)	Zr2	S3a	2.596(2)
Zr1	S2	2.592(2)	Zr2	S3b	2.596(2)
Zr1	S2a	2.592(2)	Zr2	S3c	2.596(2)
Zr1	S2b	2.592(2)	S1	P	2.0307(7)
Zr1	S2c	2.592(2)	S2	Pa	2.016(3)
Zr1	S1	2.859(2)	S3	P	1.999(3)
Zr1	S1a	2.859(2)	P	Pa'	2.227(1)

Fractional coordinates, selected bond lengths and angles, and temperature factors are listed in Tables 1–8. ZrP_2S_6 crystallized in the tetragonal space group $P-4$ with

TABLE 3
Bond Angles (Degrees) and Their Estimated Standard Deviations for ZrP_2S_6

Atom 1	Atom 2	Atom 3	Angle	Atom 1	Atom 2	Atom 3	Angle
S1	Zr1	S1a	68.32(5)	S2	Zr1	S2a	150.09(9)
S1	Zr1	S1b	133.21(3)	S2	Zr1	S2b	93.82(2)
S1	Zr1	S1c	133.21(3)	S3	Zr1	S2c	93.82(2)
S1	Zr1	S2	81.12(5)	S1	Zr1	S2b	93.82(2)
S1	Zr1	S2a	74.17(4)	S1	Zr1	S2c	93.82(2)
S1c	Zr1	S2	70.99(5)	S1	Zr1	S2c	150.09(9)
S1	Zr1	S2c	138.83(5)	S5	Zr2	S1a	69.22(6)
S1a	Zr1	S1b	133.21(3)	S5	Zr2	S1b'	132.64(4)
S1a	Zr1	S1c	133.21(3)	S6	Zr2	S1c'	132.64(4)
S1a	Zr1	S2	74.17(4)	S1	Zr2	S3	74.16(5)
S1b	Zr1	S2b	81.12(5)	S1	Zr2	S3b	81.25(5)
S1a	Zr1	S2b	138.83(5)	S1	Zr2	S3c	139.28(6)
S1b	Zr1	S2a	70.99(5)	S1	Zr2	S3a	70.65(5)
S1b	Zr1	S2c	68.32(5)	S1	Zr2	S1b'	132.64(4)
S1b	Zr1	S2	138.83(5)	S1	Zr2	S1c'	132.64(4)
S1a	Zr1	S2c	70.99(5)	S1	Zr2	S3	81.25(5)
S1c	Zr1	S2c	81.12(5)	S1	Zr2	S3b	74.16(5)
S1b	Zr1	S2c	74.17(4)	S1a	Zr2	S3c	70.56(5)
S1	Zr1	S2	70.99(5)	S1a	Zr2	S3a	139.28(6)
S1c	Zr1	S2a	138.83(5)	S1b'	Zr2	S1c'	69.22(6)
S1c	Zr1	S2b	74.17(4)	S1c'	Zr2	S3b	70.56(5)
S1a	Zr1	S2b	81.12(5)	S1b'	Zr2	S3b	139.28(6)
S1c'	Zr2	S3a	74.16(5)	Zr1	S1	Zr2	111.23(2)
S1b'	Zr2	S3a	81.25(5)	Zr1	S1	P	83.18(8)
S1c'	Zr2	S3	139.28(6)	Zr2	S1	P	83.64(8)
S1b'	Zr2	S3	70.56(5)	Zr1	S2	Pa	91.69(7)
S1c'	Zr2	S3c	81.25(5)	Zr2	S3	P	91.50(7)
S1b'	Zr2	S3c	74.16(5)	S1	P	S2a	110.0(1)
S3a	Zr2	S3c	150.06(9)	S1	P	S3	109.7(1)
S3b	Zr2	S3a	93.82(2)	S1	P	Pa'	106.80(4)
S3b	Zr2	S3c	93.82(2)	S2a	P	S3	116.08(4)
S3	Zr2	S3a	93.82(2)	S2a	P	Pa'	106.85(6)
S3	Zr2	S3c	93.82(2)	S3	P	Pa'	106.87(7)
S3	Zr2	S3b	150.06(9)				

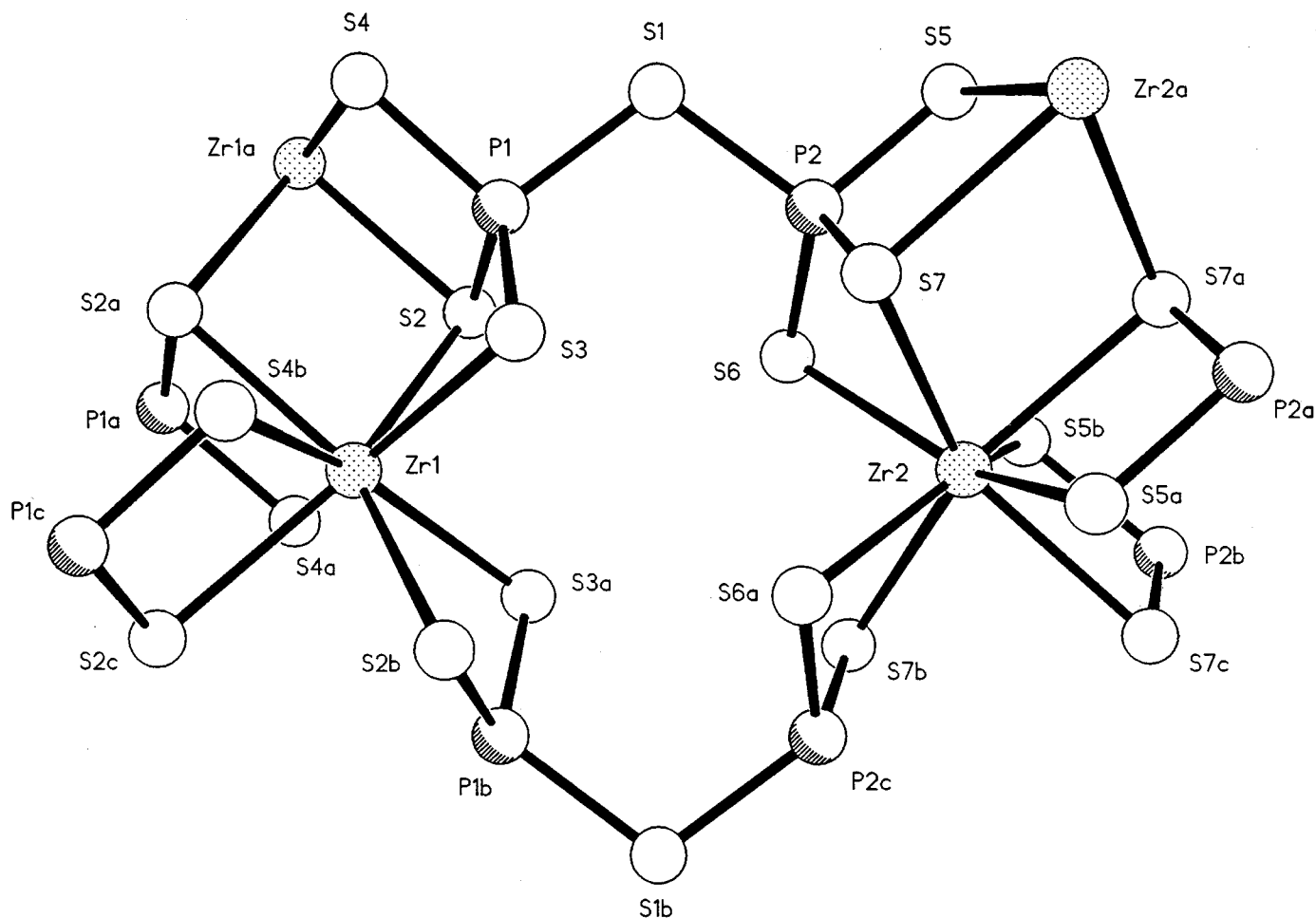


FIG. 4. Crystal structure of ZrP_2S_7 showing the coordination around the two independent Zr atoms and the $\text{P}_2\text{S}_7^{4-}$ ion including the atom number scheme used in Tables 5–8.

$a = 6.6758(4) \text{ \AA}$ and $c = 9.491(1) \text{ \AA}$, $Z = 2$. The cell volume was calculated to be 422.96 \AA^3 , and the density was calculated to be 2.71 g/cm^3 . These results are similar to those reported by Hahn *et al.* The source of the acentricity will be discussed below.

ZrP_2S_7 crystallized in the monoclinic space group $C2/c$ with $a = 8.614(1) \text{ \AA}$, $b = 29.684(4) \text{ \AA}$, $c = 8.583(1) \text{ \AA}$, and $\beta = 120.126(6)^\circ$, $Z = 8$. The cell volume was calculated to be 1898.3 \AA^3 , and the density was calculated to be 2.64 g/cm^3 .

TABLE 4
Refined Displacement Parameter Expressions (Betas) and Their Estimated Standard Deviations for ZrP_2S_6

Name	$\beta(1, 1)$	$\beta(2, 2)$	$\beta(3, 3)$	$\beta(1, 2)$	$\beta(1, 3)$	$\beta(2, 3)$
Zr1	0.00645(6)	$\beta(1, 1)$	0.00183(4)	0	0	0
Zr2	0.00471(5)	$\beta(1, 1)$	0.00206(4)	0	0	0
S1	0.00626(8)	0.00627(8)	0.00268(4)	-0.0008(1)	-0.0010(4)	0.0022(4)
S2	0.0102(1)	0.0060(1)	0.00329(6)	-0.0005(2)	-0.0064(1)	-0.0010(1)
S3	0.0091(1)	0.0084(1)	0.00340(6)	-0.0079(2)	-0.0022(1)	0.0050(1)
P	0.00696(8)	0.00413(7)	0.00203(4)	0.0001(1)	-0.0008(4)	-0.0007(4)

TABLE 5
Positional Parameters and Their Estimated Standard Deviations and the Equivalent Isotopic Temperature Factors for ZrP_2S_7

Atom	X	Y	Z	B (eq)
Zr1	0.500	0.01509(1)	0.250	0.901(8)
Zr2	0.500	0.23493(1)	0.250	0.902(8)
S1	0.2229(1)	0.12502(3)	-0.3045(1)	1.32(2)
S2	0.57117(9)	0.05284(3)	-0.00793(9)	1.08(2)
S3	0.25203(9)	0.07596(3)	0.06684(9)	1.35(2)
S4	0.18302(9)	0.01785(3)	-0.3127(1)	1.28(2)
S5	0.25428(9)	0.23214(3)	-0.31276(9)	1.28(2)
S6	0.56489(9)	0.17407(3)	0.06680(9)	1.35(2)
S7	0.17078(9)	0.19722(3)	-0.00802(9)	1.09(1)
P1	0.30343(9)	0.06818(3)	-0.13482(9)	1.03(2)
P2	0.31153(9)	0.18184(3)	-0.13515(9)	1.01(2)

The structures of ZrP_2S_6 and ZrP_2S_7 are related in that both consist of eight coordinate zirconium as shown in Figs. 3 and 4. The coordination about zirconium has been observed before in tetrakis (acetylacetonato) zirconium (13). It consists of two interpenetrating tetrahedrons resulting in a triangulated dodecahedral (bisdisphenoid) arrangement (14). The symmetry around the Zr atoms in ZrP_2S_6 is D_{2d} . In both crystal structures, one dimensional chains of edge shared ZrS_8 dodecahedron form the main structural feature. The difference between the two structures is seen in Figs. 5 and 6. In ZrP_2S_6 , the chains are all parallel to the c axis, and in ZrP_2S_7 , the chains alternate direction by 90° such that half are parallel to the c axis and half are parallel to the a axis. The space group of ZrP_2S_6 is reflected in its crystal habit: long needles with a square cross section. In ZrP_2S_6 , as seen in Fig. 5, the chains are connected through S-P-P-S bonds, and in ZrP_2S_7 (Fig. 6), the chains are connected through S-P-S-P-S bonds.

The coordination about the phosphorus in the ZrP_2S_6 compound has been observed previously. As mentioned above, the $P_2S_6^{4-}$ unit adopts an ethane-like structure with the phosphorus atoms bound to each other. Each

TABLE 6
Selected Bond Distances (\AA) and Their Estimated Standard Deviations for ZrP_2S_7

Atom 1	Atom 2	Distance	Atom 1	Atom 2	Distance
Zr1	S2	2.8098(9)	S2	P1	2.047(1)
Zr1	S3	2.6320(8)	S3	P1	2.004(1)
Zr2	S6	2.633(1)	S4	P1	2.012(1)
S1	P1	2.106(1)	S6	P2	2.0058(8)
S1	P2	2.104(1)	S7	P2	2.049(1)

TABLE 7
Bond Angles (Degrees) and Their Estimated Standard Deviations for ZrP_2S_7

Atom 1	Atom 2	Atom 3	Angle	Atom 1	Atom 2	Atom 3	Angle
S2	Zr1	S3	71.84(3)	S2	P1	S3	104.15(4)
S6	Zr2	S7	71.87(2)	S2	P1	S4	104.62(5)
P1	S1	P2	106.57(4)	S3	P1	S4	119.20(6)
Zr1	S2	P1	82.81(4)	S1	P2	S5	101.87(4)
Zr1	S3	P1	88.39(4)	S1	P2	S6	111.40(5)
Zr2	S6	P2	88.40(4)	S1	P2	S7	116.11(5)
Zr2	S7	P2	82.85(3)	S5	P2	S6	119.15(5)
S1	P1	S2	115.99(5)	S5	P2	S7	104.65(5)
S1	P1	S3	111.49(5)	S6	P2	S7	104.09(5)
S1	P1	S4	101.81(4)				

phosphorus is also connected to three sulfurs. The S-P-P-S dihedral angles are consistent with the staggered conformation expected for an ethane-like structure. This hexathiohypophosphate ion ($P_2S_6^{4-}$) is present in a number of layered $M_2P_2S_6$ materials such as $Fe_2P_2S_6$ (15). In these layered compounds, the P-P bonds are all parallel to each other, and the $P_2S_6^{4-}$ ions form two dimensional sheets. The metals occupied half of the octahedral holes defined by the sulfurs resulting in a CdI_2 -type structure.

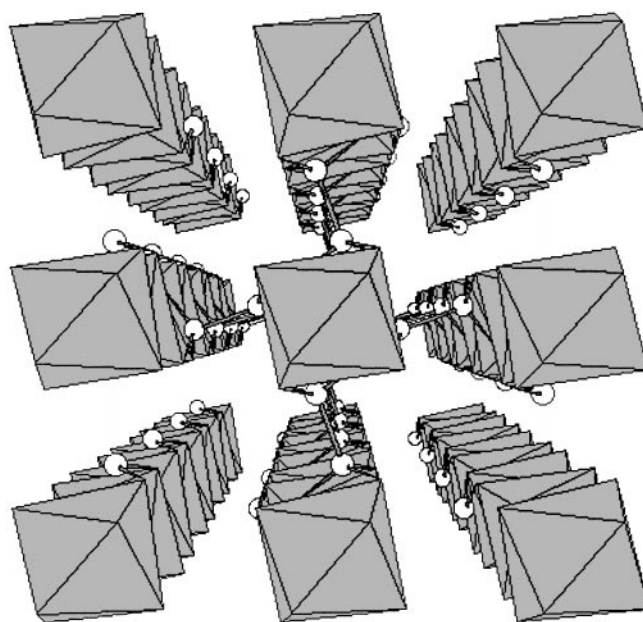


FIG. 5. Perspective drawing of ZrP_2S_6 along the c axis showing how the $P_2S_6^{4-}$ ions connect parallel chains of zirconium-sulfur dodecahedrons. The polyhedra are ZrS_8 and the open circles are phosphorus atoms.

TABLE 8
Refined Displacement Parameter Expressions (Betas) and Their Estimated Standard Deviations for ZrP_2S_7

Name	$\beta(1, 1)$	$\beta(2, 2)$	$\beta(3, 3)$	$\beta(1, 2)$	$\beta(1, 3)$	$\beta(2, 3)$
Zr1	0.00430(5)	0.00026(1)	0.00372(5)	0	0.00398(7)	0
Zr2	0.00420(5)	0.00026(1)	0.00378(5)	0	0.00391(7)	0
S1	0.0082(1)	0.00027(1)	0.00375(9)	0.00025(5)	0.0037(1)	0.00000(5)
S2	0.00461(9)	0.00033(1)	0.00453(9)	-0.00007(5)	0.0041(1)	-0.00022(4)
S3	0.00680(9)	0.00042(1)	0.00588(9)	0.00096(5)	0.0079(1)	0.00076(5)
S4	0.00455(9)	0.00034(1)	0.0063(1)	-0.00004(5)	0.0038(1)	-0.00056(5)
S5	0.00756(9)	0.00033(1)	0.00634(9)	0.00059(5)	0.0096(1)	0.00066(5)
S6	0.00491(9)	0.00042(1)	0.0060(1)	0.00022(5)	0.0044(1)	-0.00084(5)
S7	0.00536(9)	0.00032(1)	0.00471(9)	0.00013(5)	0.0056(1)	0.00022(5)
P1	0.00490(9)	0.00027(1)	0.0044(1)	0.00018(5)	0.0042(1)	0.00016(5)
P2	0.00512(9)	0.00026(1)	0.00422(9)	0.00005(5)	0.0045(1)	-0.00013(5)

The $P_2S_7^{-4}$ found in ZrP_2S_7 has also been observed before in compounds such as $Ag_4P_2S_7$, $Hg_2P_2S_7$, and $RbVP_2S_7$ (6–8). In $P_2S_7^{-4}$, each phosphorus is tetrahedrally coordinated by four sulfurs. Two PS_4 tetrahedron are linked through a common sulfur vertex to form P_2S_7 . There are no P–P bonds in ZrP_2S_7 . The sulfurs in ZrP_2S_7 bridge either two phosphorus atoms (e.g., S1) or a phosphorus and a zirconium (e.g., S3). In the case where the P–S bond is to a sulfur connecting phosphorus atoms, the bond length is longer (2.106(1) Å) than the P–S bond to sulfur connected to a zirconium (2.004(1) Å).

The difference between the acentric ZrP_2S_6 and the centrosymmetric ZrP_2S_6 is the Zr–S bond lengths. The centrosymmetric phase contains one type of Zr with long (2.875(2) Å) and short (2.599(2) Å) bonds to sulfur. The acentric phase contains two types of zirconium. Both types have long and short zirconium–sulfur bonds where the short bond length is essentially the same as that observed in the centrosymmetric phase. The difference lies in the long zirconium–sulfur bonds. The acentric material has long zirconium–sulfur bonds of 2.892(2) Å and 2.859(2) Å for the two types of zirconium compared to the centrosymmetric material's long zirconium–sulfur bond length 2.875 Å. These differences are summarized below.

	Long Zr–S bond length	Short Zr–S bond length
Centrosymmetric Zr–S	2.875(2) Å	2.599(2) Å
Acentric Zr1–S	2.892(2) Å	2.592(2) Å
Acentric Zr2–S	2.859(2) Å	2.596(2) Å

CONCLUSIONS

The compounds ZrP_2S_6 and ZrP_2S_7 were prepared and characterized by elemental analysis, infrared spectroscopy, and single crystal structure determination. The ZrP_2S_6

crystallized in an acentric space group, $P-4$, and displayed a weak second harmonic generation at 1064 nm. With ZrP_2S_6 , some of our objectives were realized. This compound was formed between a +4 metal ion and $P_2S_6^{-4}$ and displayed second harmonic generation (albeit much less than SnP_2S_6). While both SnP_2S_6 and ZrP_2S_6 contain the $P_2S_6^{-4}$ ion, ZrP_2S_6 was not a layered compound like SnP_2S_6 . In addition, ZrP_2S_6 had an eight coordinate metal ion instead of a six coordinate metal ion as is observed in SnP_2S_6 .

At the reaction temperature of 475°C, crystals of ZrP_2S_7 (orange) grew along with ZrP_2S_6 (yellow). The ZrP_2S_7 compound crystallized in the centrosymmetric space group $C2/c$ and hence displayed no second order nonlinear optical properties. Like ZrP_2S_6 , it contained eight coordinate Zr^{+4} ions, but in contrast to ZrP_2S_6 , the coordinating anion was $P_2S_7^{-4}$ instead of $P_2S_6^{-4}$.

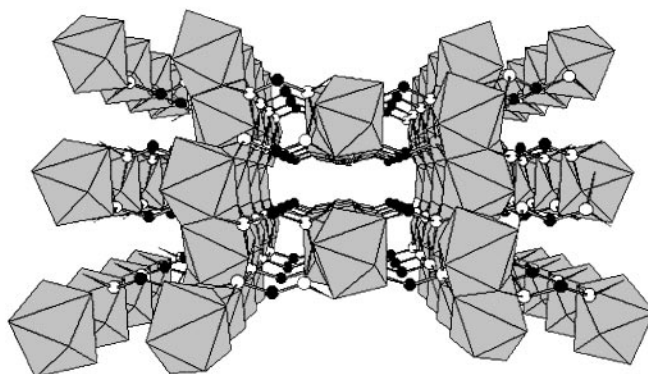


FIG. 6. Perspective drawing of ZrP_2S_7 along the c axis showing how the $P_2S_7^{-4}$ ions connect chains of zirconium–sulfur dodecahedrons. The polyhedra are ZrS_8 , the open circles are phosphorus atoms, and the filled circles are sulfur atoms. One half of the polyhedra chains are parallel to the c axis, and the other half of the chains are parallel to the a axis (vertical direction in Fig. 6).

ACKNOWLEDGMENTS

The authors acknowledge the assistance of Prof. M. Kuzyk (Washington State Univ.) with the second harmonic generation measurements. In addition, the authors acknowledge the generous support of Research Corporation and the National Science Foundation (CHE-9616316).

REFERENCES

1. R. Brec, *Solid State Ionics* **22**, 3 (1986).
2. M. S. Whittingham and A. J. Jacobson, Eds., "Intercalation Chemistry," New York, 1982.
3. P. J. S. Foot and B. A. Nevet, *Solid state Ionics* **8**, 169 (1983).
4. Z. Wang, R. D. Willett, R. A. Laitinen, and D. A. Cleary, *Chem. Mater.* **7**, 856 (1995).
5. V. A. Simon, K. Peters, E.-M. Peters, and H. Hahn, *Z. Anorg. Allg. Chem.* **491**, 295 (1982).
6. F. Menzel, L. Ohse, and W. Brockner, *Heteroat. Chem.* **1**, No. 5, 357 (1990).
7. M. Z. Jandali, G. Eulenberger, and H. Hahn, *Z. Anorg. Allg. Chem.* **445**, 184 (1978).
8. E. Durand, M. Evain, and R. Brec, *J. Solid State Chem.* **102**, 146 (1993).
9. G. M. Sheldrick, "SHELXTL/PC. Version 4.1." Siemens Analytical X-ray Instruments Inc., Madison, WI, 1990.
10. D. T. Cromer and J. B. Mann, *Acta Cryst. A* **24**, 321 (1968).
11. C. Sourisseau, J. P. Forgerit, and Y. Mathey, *J. Solid State Chem.* **49**, 134 (1983).
12. R. W. Boyd, "Nonlinear Optics," Academic Press, Boston, 1992.
13. V. W. Day and R. C. Ray, *J. Chem. Soc.* **97**, 5136 (1975).
14. A. F. Wells, "Structural Inorganic Chemistry," 5th ed., p. 79. Clarendon Press, Oxford, 1990.
15. W. Klingen, G. Eulenberger, and H. Hahn, *Z. Anorg. Allg. Chem.* **401**, 97 (1973).